

# Stochastic consideration of relationship between occurrences of earthquake and fluctuations in the radio wave propagation

Kuniyuki Motojima<sup>1</sup>, Kousuke Tanigawa<sup>1</sup>, and Nozomi Haga<sup>1</sup>

<sup>1</sup>Gunma University, 1-5-1, Tenjin-cho, Kiryu, Gunma 376-8515, Japan

*Correspondence to:* K. Motojima (motojima@gunma-u.ac.jp)

**Abstract.** Research of the geophysical electromagnetic phenomena with seismic activity is important for hazard-resistant strategy. Many papers which indicate the probable existence of geophysical electromagnetic phenomena associated with earthquakes are reported frequently. Anomalous propagation in the radio waves sometimes occurred around the same time of earthquakes. In previous paper, authors proposed a new concept to estimate the relation between earthquakes and anomalous line-of-sight propagation in VHF band by statistical approach. Event probability of the anomalous line-of-sight propagation increased just a few days prior to earthquakes. In this paper, we investigate a new relationship between anomalous fluctuations in the radio waves, which propagated from line-of-sight region, and occurrences of earthquake by using statistical analysis. Monitoring the strength of radio waves and detecting the anomalous fluctuations by using a new original method, we can obtain the high probability which indicates a possibility of association between the anomalous propagation and occurrences of earthquake. Moreover, we performed the ROC analysis for verification of our statistical result. The result of analysis indicates that our statistical results are reasonable and not artificial. After the stochastic consideration, we can find out that the anomalous fluctuations sometimes appear a few hours or days prior to earthquakes near the wave propagation path.

## 1 Introduction

There is a probable existence of some relations between earthquakes and electromagnetic phenomena in a global scale. Research of the relationship between both is very important for a country with frequent earthquakes, like Japan. There are many reports about geophysical electromagnetic phenomena associated with earthquakes. Geophysical electromagnetic phenomena can be observable by using electromagnetic wave propagation. Almost reports on the geophysical electromagnetic phenomena are classified into two groups, direct observations (Gokhberg et al., 1982; Smith et al., 1990; Hayakawa et al. 1996) or indirect observations (Fujiwara et al., 2004; Hayakawa et al., 2010).

In indirect observations, radio wave propagation is monitored for investigating the geophysical electromagnetic phenomena. The target radio waves are almost in VLF and VHF bands. Anomalous perturbation at the bottom of ionosphere can be monitored by measuring the VLF radio waves propagation. An anomaly in ionosphere appeared a few weeks prior to earthquake associated with it (Muto et al., 2009; Chakrabarti et al., 2010). Especially, some anomalies in signal amplitude and phase around sunrise and sunset times appeared a few days prior to the Kobe Japan earthquake, which occurred on 17th January 1995 (Molchanov and Hayakawa, 2007).

The other hand, there are many papers which report anomalous propagation in the VHF band waves from over-horizon broadcasting stations (Yonaiguchi et al., 2007). Yasuda et al. (Yasuda et al., 2009) reported that the anomalous propagation associated with earthquake occurred in the troposphere, and the anomaly affected the propagation path more  $100km$  or so away.

5 The purpose of our research is to find out any relation between occurrences of earthquake and anomalous line-of-sight propagation in the VHF band. We have been observed broadcasting radio waves from line-of-sight region for several years. In the previous paper (Motojima and Haga, 2014), we reported that there was a possibility of association between the anomalous propagation and earthquakes by using the statistical analysis, in which we proposed an original estimation method of probability. As the results of stochastic analysis, earthquakes occurred after anomalous propagation were characterized by magnitude  
10  $M \geq 4.5$  near the propagation path.

In this paper we propose a new detection procedure of anomalous propagation for stochastic consideration. In the new method, the fluctuations are derived from the strength of radio wave by using wavelet analysis method. As the result of new method, we can get the high probability which indicates a possibility of association between earthquakes and anomalous propagation.

## 15 2 Anomalous line-of-sight propagation in the radio waves

The purpose of this paper is to discover any relationship between anomalous fluctuations in the line-of-sight radio propagation and occurrences of earthquake. We set up an observatory of radio waves at Kiryu Japan ( $36^{\circ}25'26''N, 139^{\circ}20'58''E$ ), which is located about  $90km$  north from Tokyo. The system structure and features was described in previous paper (Motojima and Haga, 2014). The radio wave observatory can provide the data of monitoring wave strength. Some dozens of waves in VHF  
20 and UHF bands can be monitored by our observatory. In this paper some representative radio waves are analyzed and discussed in detail. The transmitter stations, path lengths from transmitting station to receiving station, names of broadcast station and frequencies are listed as Table 1. Map position of the observatory, radio transmitter stations and wave propagation paths are described in Fig. 1. Black diamond is the observatory, sold black circles are the transmitting stations. Dashed lines show the wave propagation paths.

25 In most anomalies the fluctuations are occurred simultaneously in the multiple waves. Figure 2 shows an example of synchronism detection of anomalous fluctuation in the line-of-sight radio wave propagation. Figure 2 is the observational result on 3rd March 2015 in the multidirectional broadcasting waves, which were incoming from three transmitter stations — Tokyo-tower, Miyama and Hiranohara stations — as shown in Fig. 1. Each black solid line indicates the received signal strength. Each green line indicates mean value ( $m$ ). Two blue lines mean an upper limit of ordinary propagation ( $m + 3\sigma$ ) and a lower limit  
30 of it ( $m - 3\sigma$ ), they were statistically derived from the long term observational data, from 2012 to 2015.

In each broadcasting wave, simultaneous anomalous fluctuation occurred at the same time: from 6 p.m. to 8 p.m. on 3rd May 2015. The wave from Miyama station showed most obvious anomaly, which is indicated in red dashed circles. First anomaly appeared in the predawn hours, then simultaneous anomaly occurred after sunset and was lasting until 11 p.m. An earthquake

happened subsequent to these anomalous fluctuations in a few hours later. It occurred at 23:30 LT on 3rd May 2015, 4.7 magnitude earthquake, centered in northern Kanto Plain ( $36^{\circ}25'26''N, 139^{\circ}20'58''E$ ). These anomalous fluctuations might be the precursor of the earthquake.

### 3 Wavelet analysis of received radio waves

5 In the previous paper, we adopted a criteria based on signal strength level as decision for detecting anomalous propagation. Received signal strength beyond  $(m + 3\sigma)$  or  $(m - 3\sigma)$  was regarded as anomalous data, they were the detection thresholds. However, propagated radio signal is influenced by climatic phenomena. Climatic phenomena make frequently anomalous level of received wave strength associated without earthquake. To avoid the influence of level variation, we adopt the wavelet analysis of temporal variation in received radio waves. For the purpose, operating procedure of data, that is received radio wave strength,  
10 noted as follows.

#### 1. Calculation of mean $m$ and standard deviation $\sigma$

Radio wave propagation is affected by daily variation, because sunlight promotes atmospheric convection. The atmospheric convection decreases in the difference of atmospheric refractivity between upper and lower atmosphere. Under normal condition, therefore, signal strength in daytime is slightly weak and stable, in night time signal strength is slightly  
15 strong and unstable. In order to take away that daily variation, received data is normalized separately each time slot of a day. In our procedure, a day is divided into 288 time slots of five minutes,  $0:00 \sim 0:05, 0:05 \sim 0:10, \dots, 23:55 \sim 24:00$  and the data is normalized separately each time slot. Mean value  $m$  and standard deviation  $\sigma$  of each time slot are derived through the whole observation period, about three years. Therefore, 288 mean values  $m_i$  and 288 standard deviations  $\sigma_i$  are calculated for  $i = 1, 2, \dots, 288$ .

#### 20 2. Normalized data of received wave strength

In order to detect anomalous fluctuation, normalized data is calculated from the mean of each time slot  $m_i$  in units of the standard deviation of each time slot  $\sigma_i$ , as following equation.

$$\text{Normalized data } x = \frac{(\text{Received signal data}) - (\text{Mean value } m_i \text{ of corresponding time slot } i)}{\text{Standard deviation } \sigma_i \text{ of the corresponding time slot } i} \quad (1)$$

$(i = 1, 2, \dots, 288)$

25 Equation (1) provides the corrected deviation free from the influence of daily variation.

#### 3. Wavelet transformation

Wavelet transform of the normalized data  $x$  is taken as the continuous wavelet transform (CWT). Wavelet coefficients  $W(b, a)$  is given as following.

$$W(b, a) = \frac{1}{\sqrt{a}} \int_{-\infty}^{+\infty} \psi^* \left( \frac{t-b}{a} \right) x(t) dt \quad (2)$$

where  $a$  is scale and  $b$  is translational value,  $x(t)$  is the normalized data. The  $\psi^*$  is the complex conjugate function of **Morlet mother wavelet** as shown below.

$$\psi(t) = \frac{1}{\sqrt[3]{\pi}} \exp(j\omega t) \exp\left(-\frac{t^2}{2}\right), \quad \omega = \pi \sqrt{\frac{2}{\ln(2)}} \quad (3)$$

The wavelet coefficients are complex number because the Morlet wavelet is complex number. Then, we take absolute value of the wavelet coefficients.

#### 4. Extraction of larger wavelet coefficients

Larger data in the top of 0.08% are extracted from the whole data of absolute wavelet coefficients. When a sequential larger coefficients appear in a few hours, we recognized the data as an anomalous fluctuation.

Figure 3 is an example of wavelet coefficients. Horizontal dashed line means the threshold level  $th$ , which was determined by the number of larger data. The wavelet coefficients exceeded the threshold level  $th$  three times from 14:42 to 21:16 LT on 12th Nov. 2012. Duration time of the exceeded wavelet coefficients was 6 hours and 34 minutes. We regarded it as occurrence of anomalous fluctuation.

### 4 Stochastic consideration between anomalous fluctuation and occurrence of earthquake

We will define a successive occurrence of anomalous fluctuation and earthquake within a short period of time as “ successive occurrence of anomalous fluctuation and earthquake.” However, even if there is no relation between the anomalous fluctuation and earthquake, both just happen to occur successively during a short term. Therefore, an unrelated probability  $P_{unrel}$  of successive occurrence of both phenomena has to be estimated and to be compared with probability of observational occurrence  $P_{obs}$ .

In order to derive the formula for the  $P_{unrel}$ , let's consider that only one anomaly and only one earthquake occurs under no relation during the entire observing period,  $T_{all}$ . At first, we derive a probability of NOT successive occurrence of both in defined time period  $t_{per}$ ,  $\bar{P}_{unrel}(t_{per})|_{Neq=1}$ . To simplify, time of occurrence of anomaly is fixed. The  $\bar{P}_{unrel}(t_{per})|_{Neq=1}$  is

the probability of occurrence of earthquake at complementary time period. Therefore, the  $\bar{P}_{unrel}(t_{per})|_{Neq=1}$  can be obtained as follows.

$$\bar{P}_{unrel}(t_{per})|_{Neq=1} = \frac{T_{all} - |t_{per}|}{T_{all}} \quad (4)$$

where  $t_{per}$  is the defined length of time period as successive occurrence of anomalous fluctuation and earthquake,  $T_{all}$  is the amount of observing time ( $T_{all} = 1095days$ ). Next, let's consider two earthquakes occur out of defined time period,  $t_{per}$ . It's probability is equal to the square of  $\bar{P}_{unrel}(t_{per})|_{Neq=1}$ . Because it is the conditional probability that first earthquake occurs out of  $t_{per}$  and second earthquake occurs out of  $t_{per}$  too. By the same token, when the number of earthquakes which occur out of  $t_{per}$  is  $N_{eq}$ , the probability can be obtained as next equation.

$$\bar{P}_{unrel}(t_{per})|_{Neq} = \left( \frac{T_{all} - |t_{per}|}{T_{all}} \right)^{N_{eq}} \quad (5)$$

where the  $N_{eq}$  is the number of occurrence of earthquake during the whole observation period  $T_{all}$ . The event which the anomaly and earthquakes just happen to occur successively in a defined time period  $t_{per}$  is complementary event of  $\bar{P}_{unrel}(t_{per})|_{Neq}$ . Therefore, the unrelated probability  $P_{unrel}(t_{per})$  of the successive occurrence of the anomaly and earthquakes can be obtained as follows (Motojima and Haga, 2014).

$$P_{unrel}(t_{per}) = 1 - \left( \frac{T_{all} - |t_{per}|}{T_{all}} \right)^{N_{eq}} \quad (6)$$

The probability of observational occurrence  $P_{obs}$  can be obtained from the results of observation, as follows.

$$P_{obs}(t_{per}) = \frac{N_{obs}(t_{per})}{N_{anom}} \quad (7)$$

where the  $N_{obs}(t_{per})$  is the number of successive occurrence of anomalous fluctuation and earthquake in the length of time period  $t_{per}$ . The  $N_{anom}$  is the number of occurrence of anomalous fluctuation during the whole observation period  $T_{all}$ .

The number of successive occurrence of anomalous fluctuation and earthquakes  $N_{obs}(t_{per})$  depends on the length of defined time period  $t_{per}$ , because the longer defined time period  $t_{per}$  makes the more anomalous fluctuation identified as “ successive occurrence of anomalous fluctuation and earthquake.” Besides, the unrelated probability  $P_{unrel}(t_{per})$  also depends on the  $t_{per}$ . The longer  $t_{per}$  makes the more unrelated probability  $P_{unrel}(t_{per})$  too. Therefore, we proposed an original concept of the probability gain  $PG$  for estimating the relationship between the anomalous fluctuation and earthquake in the previous paper (Motojima and Haga, 2014). The probability gain  $PG$  is the ratio of the observational probability  $P_{obs}$  to the unrelated probability  $P_{unrel}$ , it can be obtained as follows.

$$PG(t_{per}) = \frac{P_{obs}(t_{per})}{P_{unrel}(t_{per})} \quad (8)$$

If the  $PG$  closes to one, comparable probability of both the observational probability  $P_{obs}$  and the unrelated probability  $P_{unrel}$ , it means that there may be no relation between the anomalous fluctuation and earthquake.

## 5 Result and discussion

The wavelet coefficients vary depending on the scale  $a$  of mother wavelet. Moreover, the  $N_{eq}$ , which is the number of earthquakes during the whole observation period  $T_{all}$ , also varies depending on the magnitude of earthquakes, depth of hypocenter and epicenter area. Therefore, we searched the best parameters with respect to the probability gain  $PG$ . Searching parameters are the scale  $a$  of Morlet wavelet, the seismic magnitude  $M$ , depth of hypocenter  $D$ , distance  $L$  between the wave path and epicenter location. Scope of each parameter is listed in Table 2. Target broadcasting wave was NHK FM Tokyo from Sky-tree transmitting station, 82.5MHz. We calculated the probability gain  $PG$  in all combinations of parameters,  $a$ ,  $M$ ,  $D$  and  $L$ , combination number was 567. As the result of calculation in all combinations, the largest number of the probability gain  $PG$  was  $PG = 9.59$  for  $a = 9.775$ ,  $M \geq 4.5$ ,  $D \leq 50km$ ,  $L \leq 100km$  and  $t_{per} = -12$  (*hours*). It indicates that the occurrence probability of earthquake under appearance of anomalous fluctuation rise up to 9.59 times higher than no anomaly observed.

Epicentral locations are marked in Fig. 4. Red circles indicate epicenters of earthquake associated with anomalous fluctuation, and black crosses are epicenters of earthquake unaccompanied by anomaly. The size of circles are scaled to the magnitudes. Dashed oval shows equidistant curve,  $L = 100km$ , from the propagation path of Sky-tree transmitting station to Kiryu observatory.

The probability gain  $PG(t_{per})$  also varies depending on the defined length of time period  $t_{per}$  as successive occurrence of anomalous fluctuation and earthquake, because both the observational probability  $P_{obs}$  and the unrelated probability  $P_{unrel}$  change depending on the  $t_{per}$ . And so, we also calculated the probability gain  $PG(t_{per})$  with respect to  $t_{per} = -720 \sim +720$  (*hours*). The sign of  $t_{per}$  means successive occurrence of anomaly before or after earthquake. Minus is anomaly prior to earthquake, plus is the opposite. The variation of probability gain  $PG(t_{per})$  with respect to  $t_{per}$  shows in Fig. 5 for NHK FM Tokyo wave. The time step takes 6 - *hours*, because the time duration of **Morlet mother wavelet** has about 6 - *hours* in case of  $a = 9.775$ . In Fig. 5 the probability gain  $PG(t_{per})$  has a peak at  $t_{per} = -12$  (*hours*). It indicates that anomalous fluctuation appears half a day before earthquake frequently. In  $-96 \leq t_{per} \leq -6$  (*hours*) the probability gain  $PG(t_{per})$  shows about three or more. On the other hand the  $PG(t_{per})$  becomes smaller at  $t_{per} \geq +30$  (*hours*) after earthquake, it is around one. Figure 5 implies the possibility that anomalous fluctuations occur before earthquakes frequently.

We analyzed other broadcasting waves coming from other stations. The parameters  $a$ ,  $M$ ,  $D$  and  $L$  are same as the analysis for NHK FM Tokyo in Fig. 5. Table 3 shows the maximum probability gain  $PG$  and  $t_{per}$  for monitoring waves at our observatory. Incoming waves from Tokyo-tower, Sky-tree, Miyama and Hiranohara stations indicate high probability gain  $PG = 3.33 \sim 9.59$ . This result implies that the anomalous fluctuations appear on plural waves coming from multidirectional stations. Anomalous fluctuations occur in the incoming VHF waves from line-of-sight region.

Moreover, in order to verify the adequate threshold level for determining anomalous fluctuation, we conducted the ROC analysis (Fawcett, 2006) with varying the threshold level for determining anomalous fluctuation. In our verification by the

ROC graph, let the Positive instance be the day earthquake occurred, and the Negative instance be the day **NOT** occurred. For the predicted classes, let the predicted Positive instance be the day anomalous fluctuation occurred, and the predicted Negative instance be the day **NOT** occurred. Therefore, true positive rate, which is vertical axis in the ROC graph, is the ratio of the number of days both anomalous fluctuation and earthquake occurred to the number of days earthquake occurred. False positive rate, which is horizontal axis, is the ratio of the number of days anomalous fluctuation occurred without earthquake to the number of days earthquake **NOT** occurred. They can be calculated as follows.

$$\text{True Positive rate} = \frac{\text{Positives correctly classified}}{\text{Total Positives}} = \frac{\text{Number of days both anomaly and Eq. occurred}}{\text{Number of days Eq. occurred}} \quad (9)$$

$$\text{False Positive rate} = \frac{\text{Negatives incorrectly classified}}{\text{Total Negatives}} = \frac{\text{Number of days anomaly occurred without Eq.}}{\text{Number of days Eq. NOT occurred}} \quad (10)$$

Figure 6 is the ROC graph for our classification which detects the anomalous fluctuation associated with earthquake. The diagonal line in ROC graph presents strategy of randomly guessing test, which means that there is no relation between anomalous fluctuation and earthquake. When the result appears in the higher left triangle, it performs good determination, which means that there is some relation between both phenomena. The outsider from the diagonal is the better for determination. Low threshold levels for determining anomalous fluctuation are plotted in right-hand of ROC graph, and high threshold levels are plotted in left-hand. For high threshold levels the results of our determination show good performance, because they are depicted away from the diagonal. For low threshold levels the results appear around the diagonal, they are nearly random guess. We use the threshold level of wavelet coefficient  $th = 3.0$ , which is indicated by arrow in the ROC graph, Fig. 6. Results of other threshold level around  $th = 3.0$  take the position away from diagonal line too. It means that the result of  $th = 3.0$  is not particular, it is reasonable threshold level. The  $PG$  is denoted in a way similar to the ratio of true positive to random guess. Therefore, higher threshold levels, which have low random guess, indicate good result of the  $PG$ , not low threshold levels.

In order to discuss the relationship between the anomalous propagation and earthquake, we adopted other benchmarks, which were a hit rate and an alarm rate. The hit rate means a reliability of detection for anomalous fluctuations occurred with earthquakes successively. The alarm rate means a reliability of detection for earthquakes occurred with anomalous fluctuations successively. They can be obtained as following.

$$\text{Hit rate} = \frac{\text{Number of anomalous fluctuations associated with earthquakes}}{\text{Number of anomalous fluctuations}} \quad (11)$$

$$\text{Alarm rate} = \frac{\text{Number of earthquakes associated with anomalous fluctuations}}{\text{Number of earthquakes}} \quad (12)$$

Both rates are also shown for each wave in Table 3. The result of both rates indicate that our method is short of the level needed to clear the precursor of earthquake. However, high probability gain  $PG$  implies the possibility of any existence of the relationship between the anomalous fluctuations and earthquakes.

## 6 Summary

In this paper, the relationship between anomalous line-of-sight propagation and occurrences of earthquake is investigated by monitoring the fluctuations in the received wave. In order to discuss the relationship of both phenomena, we applied the new method which was the wavelet analysis of received wave. Anomalous phenomenon is contained in the shape of anomalous fluctuation of the received wave strength. Using the wavelet analysis, we can find out the anomalous fluctuation in the received wave. Then, we adopted the original evaluation method, which was calculation of the probability gain  $PG$ . The maximum probability gain  $PG$  was 9.59, which appeared in broadcast wave of NHK FM Tokyo, frequency  $f = 82.5MHz$ , from Sky-tree transmitting station. Moreover, other broadcasting waves incoming from line-of-sight region were investigated by using the wavelet analysis and the original estimation. They indicated similar number of  $PG$  for NHK FM Tokyo. It means that the anomalous propagation appears in not only specific wave (NHK FM Tokyo) but also multidirectional waves. This result suggests the possible existence of relationship between anomalous fluctuations in radio waves and occurrences of earthquake, and anomalous fluctuations sometimes appear a few hours or days prior to earthquakes.

In this paper discussion remains limited to the stochastic method only. Moreover, we can not exhibit any hypothetic model which makes the anomalous propagation associated with earthquake. However, our statistical consequence dose not deny the possible existence of any relationship between the anomalous propagation in radio wave and earthquake. We hope that our results can benefit the research of geophysical electromagnetic phenomena associated with earthquakes.

We investigated only a few wavelet analysis methods. Many analysis methods have not been tried yet. These are in future works.

*Acknowledgements.* This work was partially supported by JSPS KAKENHI Grant Number 26420382. Earthquake Information of Japan Meteorological Agency was referred for our statistical investigation.



## References

- Chakrabarti, S. K., Sasmal, S., and Chakrabarti S.: Ionospheric anomaly due to seismic activities - Part 2: Evidence from D-layer preparation and disappearance times, *Nat., Hazards Earth Syst. Sci.*, 10, 1751-1757, doi:10.5194/nhess-10-1751-2010, 2010.
- Fawcett Tom: An introduction to ROC analysis, *Pattern Rec. Lett.*, 27, 861-874, doi:10.1016/j.patrec.2005.10.010, 2006.
- 5 Fujiwara, H., Kamogara, M., Ikeda, M., Liu, J. Y., Sakata, H., Chen, Y. I., Ofuruton, H., Muramatsu, S., Chuo, Y. J., and Ohtsuki, Y. H.: Atmospheric anomalies observed during earthquake occurrences, *Geophys. Res. Lett.*, 31, L17110, doi:10.1029/2004GL019865, 2004.
- Gokhberg, M. B., Morgounov, V. A., Yoshino, T., and Tomizawa, I.: Experimental measurement of electromagnetic emissions possibly related to earthquakes in Japan, *J. Geophys. Res.*, 87, 7824-7828, 1982.
- Hayakawa, M., Kawate, R., Molchanov, O. A., and Yumoto, K.: Results of ultra-low-frequency magnetic field measurements during the  
10 Guam earthquake of 8 August 1993, *Geophys. Res. Lett.*, 23, 241-244, doi:10.1029/95GL02863, 1996.
- Hayakawa, M., Kasahara, Y., Nakamura, T., Muto, F., Horie, T., Maekawa, S., Hobara, Y., Rozhnoi, A. A., Solovieva, M., and Molchanov, O., A.: A Statistical study on the correlation between lower ionospheric perturbations as soon by subionospheric VLF/LF propagation and earthquakes, *J. Geophys. Res.*, 115, A09305, doi:10.1029/2009JA015143, 2010.
- Molchanov, O. A., and Hayakawa, M.: Subionospheric VLF signal perturbations possibly related to earthquakes, *J. Geophys. Res.*, 103,  
15 17489-17504, doi:10.1029/98JA00999, 1998.
- Motojima K., and Haga N.: Stochastic relation between anomalous propagation in the line-of-sight VHF radio band and occurrences of earthquakes, *Nat., Hazards Earth Syst. Sci.*, 14, 2119-2124, doi:10.5194/nhess-14-2119-2014, 2014.
- Muto, F., Kasahara, Y., Hobara, Y., Hayakawa, M., Rozhnoi, A., Solovieva, M., and Molchanov, O. A.: Further study on the role of atmospheric gravity waves on the seismo-ionospheric perturbations as detected by subionospheric VLF/LF propagation, *Nat., Hazards Earth  
20 Syst. Sci.*, 9, 1111-1118, 2009.
- Smith, A. C. F., Bernardi, A., McGill, P. R., Ladd, M. E., Helliwell, R. A., and Villard, O. G. Jr.: Low-frequency magnetic field measurements near the epicenter of the Ms 7.1 Loma Prieta earthquake, *Geophys. Res. Lett.*, 17, 1465-1468, doi:10.1029/GL017i009p01465, 1990.
- Yasuda, Y., Ida, Y., Goto, T., and Hayakawa, M.: Interferometric direction finding of over-horizon VHF transmitter signals and natural VHF radio emissions possibly associated with earthquakes, *Radio Sci.*, 44, RS2009, doi:10.1029/2008RS003884, 2009.
- 25 Yonaiguchi, N., Ida, Y. and Hayakawa, M.: On the statistical correlation of over-horizon VHF signals with meteorological radio ducting and seismicity, *J. Atmos. Solar-terr. Phys.*, 69, 661-674, doi:10.1016/j.jastp.2007.01.007, 2007.

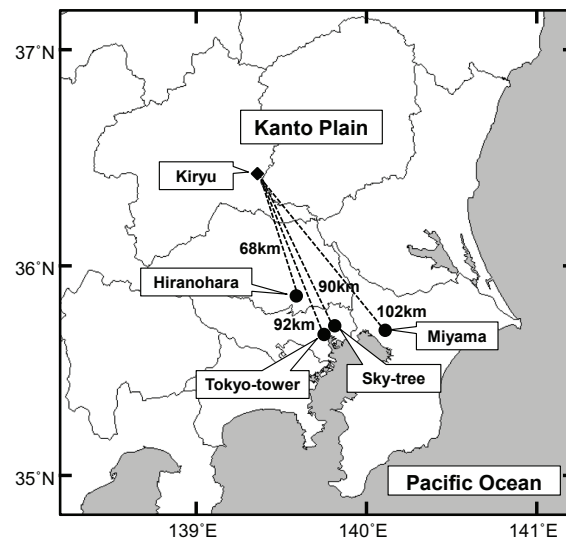


**Figure 1.** Map of observatory, transmitter stations and wave propagation paths. Black diamond is the observatory, solid black circles are the transmitter stations. Dashed lines show the wave propagation paths.

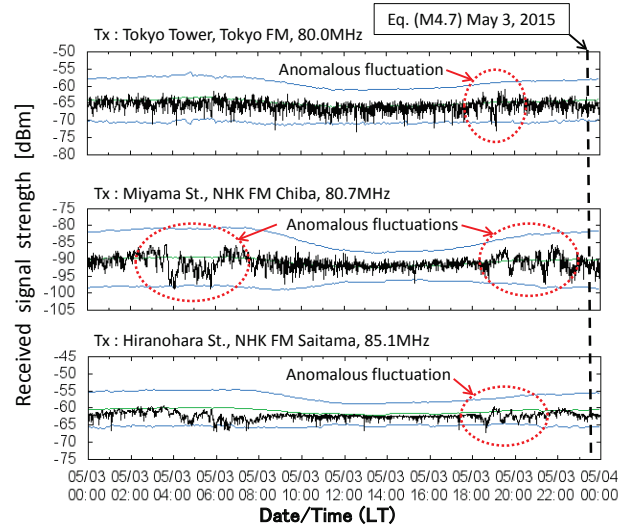


**Figure 2.** An example of synchronism detection of anomalous fluctuations in the line-of-sight stations on 3rd May 2015. Each green line indicates mean value ( $m$ ), two blue lines mean an upper limit of ordinary propagation ( $m + 3\sigma$ ) and a lower limit of it ( $m - 3\sigma$ ). Earthquake occurred at 23:30 LT on 3rd May 2015, seismic magnitude 4.7, epicenter ( $36^{\circ}25'26''N$ ,  $139^{\circ}20'58'E$ ) in northern Kanto Plain.

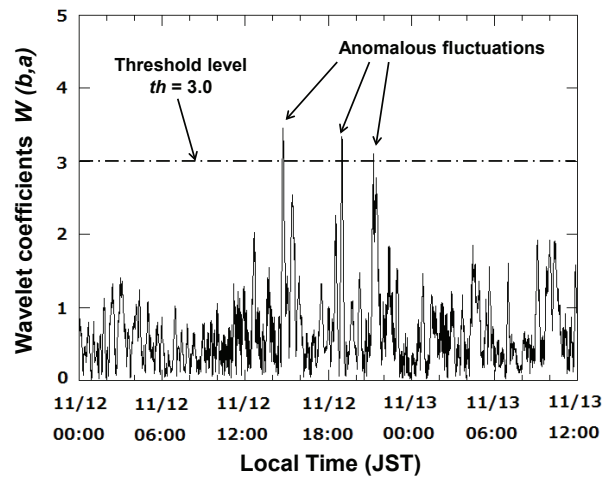


**Figure 3.** An example of anomalous fluctuation in wavelet coefficients  $W(b, a)$  from 12th to 13th Nov. 2012. Scale of mother wavelet  $a = 9.775$ , threshold level 3.0.

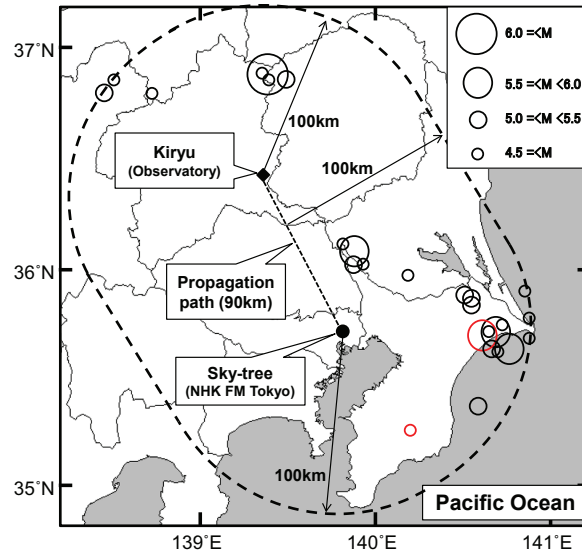


**Figure 4.** Epicentral locations. Red circles indicate epicenters of earthquake associated with anomalous fluctuation, and black crosses are epicenters of earthquake unaccompanied by anomaly. The size of circles are scaled to the magnitudes. Dashed oval shows equidistant curve,  $L = 100\text{km}$ , from the propagation path of Sky-tree transmitting station to Kiryu observatory.

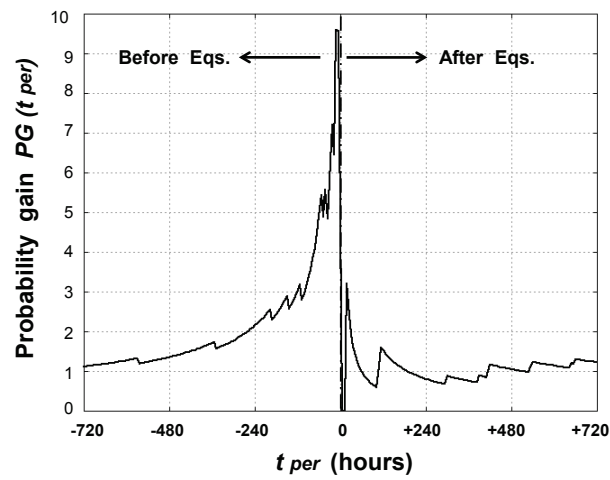


**Figure 5.** The probability gain  $PG(t_{per})$  for NHK FM Tokyo wave. Scale of mother wavelet  $a = 9.775$ , seismic magnitude  $M \geq 4.5$ , depth of hypocenter  $D \leq 50km$ , distance between the wave path and epicenter location  $L \leq 100km$ .

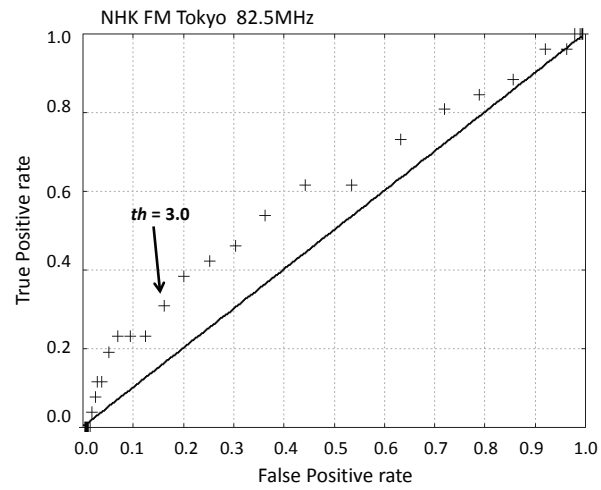


**Figure 6.** The ROC graph for our classification which detects the anomalous fluctuation associated with earthquake. True positive rate is the ratio of the number of days both anomaly and EQ occurred to the number of days EQ occurred. False positive rate is the ratio of the number of days anomaly occurred without EQ to the number of days EQ NOT occurred.

**Table 1.** The transmitter stations, path lengths from Tx to Rx, names of broadcast station and transmit frequency.

Transmitter station	Path length from Tx. to Rx.	Name of broadcast station	Transmit frequency
Tokyo tower (Tokyo)	$92km$	FM Tokyo	$80.0MHz$
		The Open Univ. of Japan	$77.1MHz$
		Inter FM	$89.7MHz$
Sky tree (Tokyo)	$90km$	NHK FM Tokyo	$82.5MHz$
		Jwave	$81.3MHz$
Miyama St. (Chiba Pref.)	$102km$	NHK FM Chiba	$80.7MHz$
		Bay FM	$78.0MHz$
Hiranohara St. (Saitama Pref.)	$68km$	NHK FM Saitama	$85.1MHz$
		TV Saitama	$587MHz$



**Table 2.** Searching parameters with respect to the probability gain  $PG$ , NHK FM Tokyo,  $f = 82.5MHz$ .

Parameter	Scope of parameters	Number of kinds
Scale of mother wavelet $a$	$4.887 \sim 156.4$	21
Seismic magnitude $M$	$M \geq 4.5, M \geq 5.0, M \geq 5.5$	3
Depth of hypocenter $D$	$D \leq 50km, D \leq 75km, D \leq 100km$	3
Distance between wave path path and epicenter location $L$	$L \leq 50km, L \leq 100km, L \leq 150km$	3

**Table 3.** The probability gain  $PG$ , the number of earthquake  $N_{eq}$ , the number of anomalous fluctuation  $N_{anom}$ , the number of successive occurrence of anomalous fluctuation and earthquake  $N_{obs}$ ,  $Hit\ rate$  and  $Alarm\ rate$  (  $a = 9.775$ ,  $M \leq 4.5$ ,  $D \leq 50km$ ,  $L \leq 100km$ ).

Broadcast station name	Transmitting station (Radion path length)	$N_{eq}$	$N_{anom}$	$N_{obs}$	$PG$ ( $t_{per}$ )	$Hit\ rate$	$Alarm\ rate$
NHK FM Tokyo	Sky tree (92km)	27	17	2	9.59 (-12 hours)	0.176	0.111
FM Tokyo	Tokyo tower (90km)	24	28	4	3.33 (-48 hours)	0.0714	0.083
NHK FM Saitama	Hiranohara St. (68km)	22	23	1	8.68 ( -6 hours)	0.087	0.091
NHK FM Chiba	Miyama St. (68km)	37	29	2	8.20 ( -6 hours)	0.138	0.081